TE_{11} to HE_{11} Cylindrical Waveguide Mode Converters Using Ring-Loaded Slots

GRAEME L. JAMES AND BRUCE M. THOMAS, SENIOR MEMBER, IEEE

Abstract—A theoretical parameter study is given of a TE_{11} to HE_{11} mode converter consisting of a section of cylindrical corrugated waveguide with ring-loaded slots. The analysis, using modal field-matching techniques to determine the scatter matrix of the converter, allows the return loss to be computed accurately. For a wide range of waveguide sizes it is shown that a bandwidth ratio of 1.5 with a return loss better than 30 dB is possible. The low-frequency performance of the converter is limited by the deterioration in return loss, while at high frequencies the generation of a small amount of unwanted EH_{12} mode is the restriction. If the effects of this mode can be neglected, operation over a wider bandwidth is possible, particularly for larger waveguide size.

I. Introduction

MATCHING OF A corrugated waveguide to a smooth-walled guide requires a transition section in which the longitudinal surface reactance inside the waveguide changes gradually from zero at the smooth-walled input-waveguide to the high value required in the corrugated output-waveguide. A common method of achieving this is to use a corrugated waveguide transition section in which the depth of the slots gradually decreases from an initial value of $\lambda/2$ (so that the input slot appears as a short circuit) to a final slot-depth of approximately $\lambda/4$ as given by the corrugated output-waveguide. In a companion paper [1], James described the use of modal field-matching techniques in analyzing the performance of this type of transition section for TE_{11} to HE_{11} mode conversion in cylindrical waveguides. Such converters, however, have a limited high-frequency performance owing to the excitation of unwanted modes, mainly at the position of the relatively deep input slot. This problem is discussed in some detail in Section III.

To increase the bandwidth performance of corrugated waveguide mode converters, Takeichi *et al.* [2] developed a cylindrical ring-loaded corrugated waveguide with slots as shown in Fig. 1(a). Making the assumption that only the dominant mode exists in the slots, they showed the impedance of a ring-loaded slot to be capacitive[1] over a considerably wider bandwidth than that achieved by a conventional constant-width slot having the same radial depth. This feature of the ring-loaded slot was used in a TE_{11} to HE_{11} mode converter in a cylindrical waveguide [2] and subsequently in matching a small-angle ring-loaded corrugated conical horn [3]. Although few details of the ring-loaded mode converter are given in [2] and a detailed analysis is not undertaken, the example does illustrate the wide bandwidth performance capability of this type of converter.

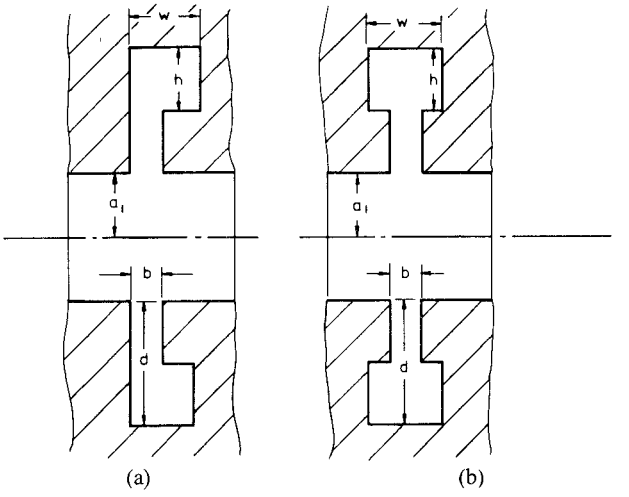

Fig. 1. Cross-sectional view of (a) asymmetrical and (b) symmetrical slots in a ring-loaded corrugated waveguide.

The purpose of this paper is to extend the previous analysis [1] to include ring-loaded slots, thereby allowing a detailed theoretical parametric study of ring-loaded slot mode converters to be undertaken. In particular, we are interested in investigating the factors affecting the low-frequency and high-frequency performance of the converter, the excitation of unwanted higher order modes, and arriving at general design data for optimum mode conversion in cylindrical waveguides. Furthermore, our analysis covers the case of the symmetrical ring-loaded slot (Fig. 1(b)) as well as the asymmetrical slot (Fig. 1(a)) used in [2] and [3].

II. Formulation

The mode converter to be analyzed is shown in Fig. 2(a), where, following the smooth-walled cylindrical input-waveguide supporting the TE_{11} mode, there is a section containing L ring-loaded slots. The dimensions of these slots and the separation between them are to be determined from our analysis in optimizing the conversion to the HE_{11} mode in the corrugated output waveguide following the Lth slot. As in [1], we first determine the individual scatter matrices for each of the changes in waveguide cross section

Manuscript received August 19, 1981; revised October 29, 1981.

The authors are with the Division of Radiophysics, Commonwealth Scientific and Industrial Research Organization, Sydney, Australia.

[1]Restriction to the capacitive region is based on the assumption that excitation of slow (surface) waves is avoided: see Section III.

0018-9480/82/0300-0278$00.75 ©1982 IEEE

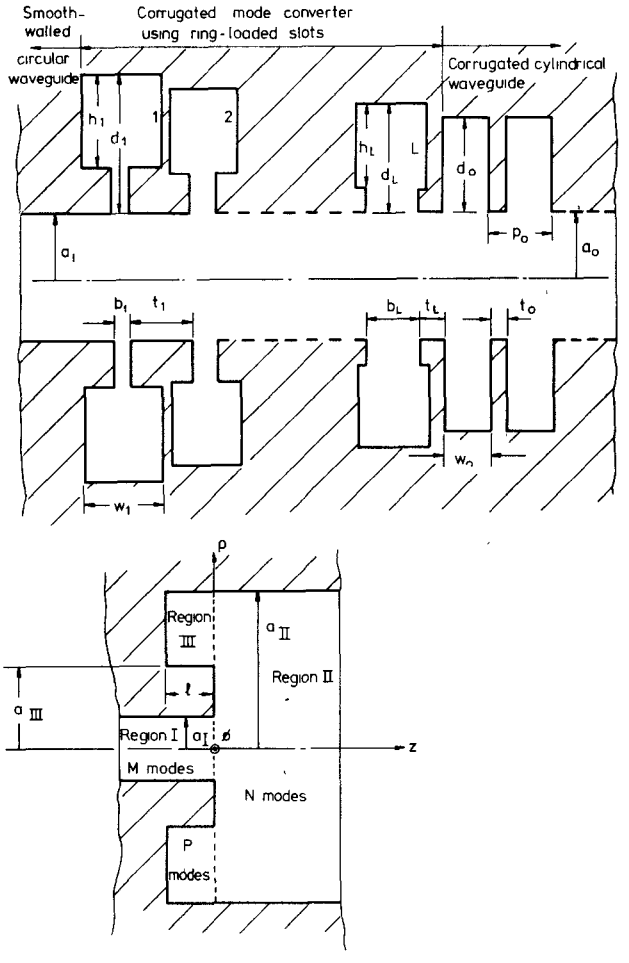

Fig. 2. Cross-sectional view of (a) corrugated mode converter section, consisting of L symmetrical ring-loaded slots placed between a smooth-walled and corrugated waveguide, and (b) junction between two smooth-walled waveguides and a short-circuited annular ring.

and for each of the short lengths of waveguide separating them which go to make up the ring-loaded slots and flanges of the corrugated transition section. Then by progressively cascading the scatter matrices through this section we obtain an overall scatter matrix from which to determine the propagation properties of the mode converter. To avoid unnecessary duplication we will rely heavily on the formulation presented in the companion paper [1].

In the analysis for the transition section containing conventional slots, it was necessary to determine the scatter matrix for the junction between two cylindrical waveguides of differing radii. The equivalent problem for the ring-loaded slots involves the more complicated waveguide junction shown in Fig. 2(b). Regions I and II are smooth-walled cylindrical waveguides, whereas region III is a short-circuited smooth-walled annular ring of depth l and radial width $a_{II} - a_{III}$. In region I the transverse field $\boldsymbol{E}_I, \boldsymbol{H}_I$ at $z=0$ is given by

$$\boldsymbol{E}_I = \sum_{m=1}^{M} (A_{mI} + B_{mI})\boldsymbol{e}_{mI}$$

$$\boldsymbol{H}_I = \sum_{m=1}^{M} (A_{mI} - B_{mI})\boldsymbol{h}_{mI} \tag{1}$$

where $\boldsymbol{e}_{mI}, \boldsymbol{h}_{mI}$ are the transverse modal fields and A_{mI}, B_{mI} are the modal coefficients to be determined. Similarly for region II at $z=0$

$$\boldsymbol{E}_{II} = \sum_{n=1}^{N} (A_{nII} + B_{nII})\boldsymbol{e}_{nII}$$

$$\boldsymbol{H}_{II} = \sum_{n=1}^{N} (A_{nII} - B_{nII})\boldsymbol{h}_{nII} \tag{2}$$

and for region III at $z=0$

$$\boldsymbol{E}_{III} = \sum_{p=1}^{P} A_{pIII}\boldsymbol{e}_{pIII}$$

$$\boldsymbol{H}_{III} = \sum_{p=1}^{P} A_{pIII}\boldsymbol{h}_{pIII}. \tag{3}$$

With TE_{11} mode excitation in the input guide (region I of Fig. 2(b)), TE_{1p} and TM_{1p} modes can be excited at each discontinuity. These transverse modal fields for regions I and II are described in [1]. For region III the solution for the TE_{1p} modes is

$$\frac{1}{\eta}\boldsymbol{e}_{pIII} = \left[\frac{G(V_p)}{V_p}\hat{\boldsymbol{\rho}}\sin\phi + G'(V_p)\hat{\boldsymbol{\phi}}\cos\phi\right]\sin y_p l$$

$$\boldsymbol{h}_{pIII} = \left[G'(V_p)\hat{\boldsymbol{\rho}}\cos\phi - \frac{G(V_p)}{V_p}\hat{\boldsymbol{\phi}}\sin\phi\right]\frac{y_p\cos y_p l}{jk} \tag{4}$$

where

$$k = 2\pi/\lambda, \qquad \eta = \sqrt{\mu/\epsilon}$$

and

$$G(V_p) = J_1(V_p)Y_1'(X_p a_{III}/a_{II}) - J_1'(X_p a_{III}/a_{II})Y_1(V_p)$$

$$V_p = X_p\rho/a_{II}$$

and

$$y_p = \sqrt{k^2 - (X_p/a_{II})^2}$$

X_p being the roots of the characteristic equation $G'(X_p)=0$. The solution for the TM_{1p} modes in region III is

$$\frac{1}{\eta}\boldsymbol{e}_{pIII} = \left[H'(V_p)\hat{\boldsymbol{\rho}}\sin\phi + \frac{H(V_p)}{V_p}\hat{\boldsymbol{\phi}}\cos\phi\right]\frac{y_p\sin y_p l}{jk}$$

$$\boldsymbol{h}_{pIII} = \left[-\frac{H(V_p)}{V_p}\hat{\boldsymbol{\rho}}\cos\phi + H'(V_p)\hat{\boldsymbol{\phi}}\sin\phi\right]\cos y_p l \tag{5}$$

where

$$H(V_p) = J_1(V_p)Y_1(X_p a_{III}/a_{II}) - J_1(X_p a_{III}/a_{II})Y_1(V_p)$$

X_p being the roots of the characteristic equation $H(X_p)=0$.

Let s_I, s_{II}, and s_{III} be the cross-sectional areas at $z=0$ of the regions I, II, and III. Then by making use of the orthogonality of the waveguide modes, the continuity of fields over s_I and s_{III}, the boundary conditions over $s_{II} - s_I - s_{III}$, we obtain the following set of simultaneous matrix

equations:

$$\begin{aligned}\underline{\underline{P}}[\underline{A}_{\mathrm{I}}+\underline{B}_{\mathrm{I}}]+\underline{\underline{U}}\underline{A}_{\mathrm{III}}&=\underline{\underline{Q}}[\underline{A}_{\mathrm{II}}+\underline{B}_{\mathrm{II}}]\\ \underline{\underline{P}}^{T}[\underline{B}_{\mathrm{II}}-\underline{A}_{\mathrm{II}}]&=\underline{\underline{R}}[\underline{A}_{\mathrm{I}}-\underline{B}_{\mathrm{I}}]\\ \underline{\underline{U}}^{T}[\underline{B}_{\mathrm{II}}-\underline{A}_{\mathrm{II}}]&=\underline{\underline{W}}\underline{A}_{\mathrm{III}}\end{aligned}\tag{6}$$

where $\underline{A}_{\mathrm{I}}$, $\underline{B}_{\mathrm{I}}$ are column matrices of M elements containing the unknown modal coefficients of region I. Similarly $\underline{A}_{\mathrm{II}}$, $\underline{B}_{\mathrm{II}}$ are column matrices of N elements and $\underline{A}_{\mathrm{III}}$ a column matrix of P elements containing the unknown model coefficients in regions II and III. $\underline{\underline{P}}$ is an $N\times M$ matrix, $\underline{\underline{U}}$ an $N\times P$ matrix, and $\underline{\underline{Q}}$, $\underline{\underline{R}}$, and $\underline{\underline{W}}$ are diagonal matrices of dimension $N\times N$, $M\times M$, and $P\times P$, respectively. The elements in these last five matrices are given by

$$\begin{aligned}P_{mn}&=\int_{s_{\mathrm{I}}}\boldsymbol{e}_{m\mathrm{I}}\times\boldsymbol{h}_{n\mathrm{II}}\cdot d\boldsymbol{s}\\ U_{pn}&=\int_{s_{\mathrm{III}}}\boldsymbol{e}_{p\mathrm{III}}\times\boldsymbol{h}_{n\mathrm{II}}\cdot d\boldsymbol{s}\\ Q_{nn}&=\int_{s_{\mathrm{II}}}\boldsymbol{e}_{n\mathrm{II}}\times\boldsymbol{h}_{n\mathrm{II}}\cdot d\boldsymbol{s}\\ R_{mm}&=\int_{s_{\mathrm{I}}}\boldsymbol{e}_{m\mathrm{I}}\times\boldsymbol{h}_{m\mathrm{I}}\cdot d\boldsymbol{s}\\ W_{pp}&=\int_{s_{\mathrm{III}}}\boldsymbol{e}_{p\mathrm{III}}\times\boldsymbol{h}_{p\mathrm{III}}\cdot d\boldsymbol{s}.\end{aligned}\tag{7}$$

The integrals in (7) can all be evaluated analytically, and the results for P_{mn}, Q_{nn}, and R_{mm} are given in [1]. For the evaluation of the remaining integrals, let $X_{p\mathrm{III}}$ represent alternately the roots of the characteristic equations for the TE and TM modes in region III (i.e., p is odd for TE modes and even for the TM modes). Similarly, let $X_{n\mathrm{II}}$ give the roots alternately for the TE and TM modes in region II with $u=X_{n\mathrm{II}}a_{\mathrm{III}}/a_{\mathrm{II}}$ the evaluation of U_{pn} and W_{pp} then becomes

$$U_{pn}=\frac{2j\eta a_{\mathrm{II}}^{2}\sin y_p l}{X_{p\mathrm{III}}^{2}-X_{n\mathrm{II}}^{2}}\begin{cases}\left[\{X_{n\mathrm{II}}/(ka_{\mathrm{II}})\}^{2}-1\right]^{1/2}J_1'(u) & (p,n=1,3,5\cdots)\\ y_p X_{n\mathrm{II}}J_1(u)/(kX_{p\mathrm{III}}) & (p,n=2,4,6\cdots)\\ j\left[1-\left(\dfrac{X_{n\mathrm{II}}}{X_{p\mathrm{III}}}\right)^{2}\right]\dfrac{J_1(u)}{u} & (p=1,3,5\cdots)\quad(n=2,4,6\cdots)\\ 0 & (p=2,4,6\cdots)\quad(n=1,3,5\cdots)\end{cases}\tag{8}$$

$$W_{pp}=(-1)^{p}\frac{\eta\pi y_p a_{\mathrm{II}}^{2}\sin 2y_p l}{4jkX_{p\mathrm{III}}^{2}}\begin{cases}\left(X_{p\mathrm{III}}^{2}-1\right)G^{2}\left(X_{p\mathrm{III}}\right)-\dfrac{4}{\pi^{2}}\left[1-\left(\dfrac{a_{\mathrm{II}}}{X_{p\mathrm{III}}a_{\mathrm{III}}}\right)^{2}\right] & (p=1,3,5\cdots)\\ \left[X_{p\mathrm{III}}H'\left(X_{p\mathrm{III}}\right)\right]^{2}-\dfrac{4}{\pi^{2}} & (p=2,4,6\cdots)\end{cases}.\tag{9}$$

In our application of (9), the dimensions of the annular slot will allow only the dominant TE_{11} mode to propagate. For the cutoff modes the value of $X_{p\mathrm{III}}$ becomes large (being given asymptotically by $p\pi a_{\mathrm{II}}/(a_{\mathrm{II}}-a_{\mathrm{III}})$). The expression for W_{pp} then becomes

$$W_{pp}\sim(-1)^{p+1}\eta\frac{(a_{\mathrm{II}}-a_{\mathrm{III}})^{2}}{ka_{\mathrm{III}}p\pi^{2}}\sin\left(\frac{2p\pi l}{a_{\mathrm{II}}-a_{\mathrm{III}}}\right)\text{ as }X_{p\mathrm{III}}\to\infty.\tag{10}$$

Returning to (6) and rearranging into the scattering matrix formulation between the input guide (region I) and output guide (region II)

$$\begin{bmatrix}\underline{B}_{\mathrm{I}}\\ \underline{B}_{\mathrm{II}}\end{bmatrix}=\begin{bmatrix}\underline{\underline{S}}_{11} & \underline{\underline{S}}_{12}\\ \underline{\underline{S}}_{21} & \underline{\underline{S}}_{22}\end{bmatrix}\begin{bmatrix}\underline{A}_{\mathrm{I}}\\ \underline{A}_{\mathrm{II}}\end{bmatrix}\tag{11}$$

we have the scattering matrix element given by

$$\begin{aligned}\underline{\underline{S}}_{11}&=[\underline{\underline{R}}+\underline{\underline{P}}^{T}\underline{\underline{F}}^{-1}\underline{\underline{P}}]^{-1}[\underline{\underline{R}}-\underline{\underline{P}}^{T}\underline{\underline{F}}^{-1}\underline{\underline{P}}]\\ \underline{\underline{S}}_{12}&=[\underline{\underline{R}}+\underline{\underline{P}}^{T}\underline{\underline{F}}^{-1}\underline{\underline{P}}]^{-1}[\underline{\underline{P}}^{T}+\underline{\underline{P}}^{T}\underline{\underline{F}}^{-1}(2\underline{\underline{Q}}-\underline{\underline{F}})]\\ \underline{\underline{S}}_{21}&=2[\underline{\underline{F}}+\underline{\underline{P}}\underline{\underline{R}}^{-1}\underline{\underline{P}}^{T}]^{-1}\underline{\underline{P}}\\ \underline{\underline{S}}_{22}&=-[\underline{\underline{F}}+\underline{\underline{P}}\underline{\underline{R}}^{-1}\underline{\underline{P}}^{T}]^{-1}[2\underline{\underline{Q}}-\underline{\underline{F}}-\underline{\underline{P}}\underline{\underline{R}}^{-1}\underline{\underline{P}}^{T}]\end{aligned}\tag{12}$$

where

$$\underline{\underline{F}}=\underline{\underline{Q}}-\underline{\underline{U}}\underline{\underline{W}}^{-1}\underline{\underline{U}}^{T}.$$

This equation gives the scattering matrix elements for the geometry in Fig. 2(b), assuming that transmission through the discontinuity is from region I to region II. In the ring-loaded slot analysis we also require the reverse situation, i.e., transmission from the ring-loaded larger guide to the smaller guide. In this case, (11) and (12) still apply but with the scatter matrix elements in (11) exchanged diagonally.

In analyzing the transition section with ring-loaded slots (Fig. 2(a)), we now proceed as in [1] but with (6) in that paper being replaced by (12) above. (Note that when the annular ring is absent, either with $l=0$ or $a_{\mathrm{III}}=a_{\mathrm{II}}$, $\underline{\underline{U}}\underline{\underline{W}}^{-1}\underline{\underline{U}}^{T}=\underline{\underline{0}}$, so that $\underline{\underline{F}}=\underline{\underline{Q}}$ and (12) reduces, as required, to the solution given by (6) in [1].) The only remaining problem is to establish the number of modes P in the

annular slots which need to be considered to ensure satisfactory convergence of the solution. In our case, with only the dominant TE_{11} mode able to propagate in the annular slots, it was found that no discernible change in the results occurred for $P>3$. Hence we put $P=3$ throughout.

III. Excitation of Higher Order Modes

The theoretical treatment developed in the above section has been used to calculate the performance of mode converters using ring-loaded corrugations. In Section IV, the performance of this type of converter will be considered in detail and compared with the converter using constant-width varying-depth slots [1]. Before doing this, however, it is useful to introduce the mode chart for a cylindrical waveguide with an anisotropic surface [4]. This chart will be used to show the conditions under which higher order mode generation may occur in both types of converters and in the corrugated output waveguide.

The mode chart appropriate for corrugated cylindrical waveguides in which the circumferential component of surface reactance is zero is shown in Fig. 3. Here the normalized propagation constant k_z/k is plotted against ka, with the longitudinal surface reactance X_z (normalized relative to free-space impedance) as parameter. For convenience, the inverse k/k_z is used in the slow-wave region. The balanced HE_{1n} and balanced EH_{1n} modes occur when $X_z=\infty$ and these become the TE_{1n} and TM_{1n} modes when $X_z=0$. The solid curve ABC in Fig. 3 is the contour of k_z/k for the HE_{11} mode in a corrugated output waveguide where the radius $a=a_o$, slot width-to-pitch ratio δ is 0.75 and where the mode is assumed balanced at a frequency f_0 corresponding to $k_0a_o=2.9$ (point B). If the frequency f is reduced below f_0 (ka_o decreasing) X_z becomes inductive, and the HE_{11} mode rapidly approaches cutoff (point A). For $f>f_0$ (ka_o increasing) the surface reactance is capacitive and gradually decreases to zero at point C ($ka_o=5.1$). Here the slot depth is $\lambda/2$ and the mode of propagation is TE_{11}. The other solid curve DE is the contour of k_z/k for the unwanted EH_{12} mode for the same set of waveguide parameters. At E we have $X_z=0$ and the mode is TM_{11}. The value of ka_o at cutoff for the EH_{12} mode (which in this example occurs at $ka_o=4.2$ (point D)) increases or decreases as k_0a_o increases or decreases: see columns 1 and 3 of Table I. If it is essential to have only the HE_{11} mode propagating in the output waveguide, operation should be restricted to the region to the left of D. When operating in the region between A and B where X_z is inductive, the surface-wave can propagate if excited. In practice, however, the surface wave excitation is not significant unless the HE_{11} mode is near cutoff.

The excitation of higher order modes at the input of the converter will now be considered, since it is at this discontinuity that the greatest mismatch is most likely to occur. For the conventional converter, the input slot depth is $\lambda/2$ at a frequency f_i, which is usually equal to $\sim 1.2f_0$. The reactance variation of this slot with frequency is then

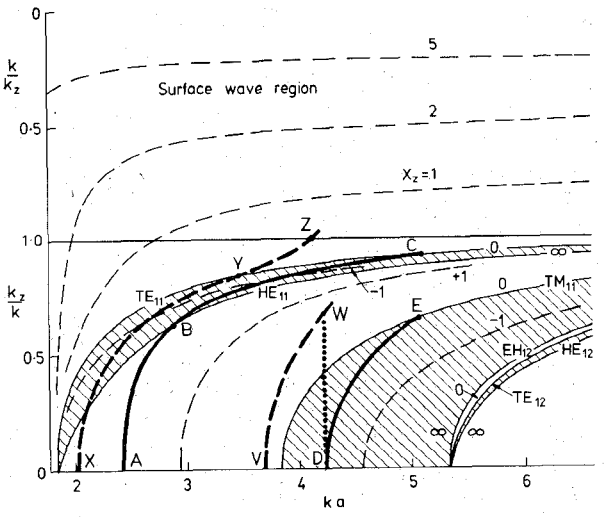

Fig. 3. Mode chart for cylindrical waveguide having anisotropic surface, where the circumferential component of surface reactance is zero, and the longitudinal surface reactance X_z is finite. The shaded areas indicate negative X_z. The first-order solutions for two corrugated waveguide systems are: —— output waveguide: $\delta=0.75$, with $X_z=\infty$ at $k_0a_o=2.9$; ---- input slot ($\lambda/2$ at k_i) of conventional converters: $\delta=0.75$, with $X_z=0$ at $k_ia_i=3.48$.

TABLE I
Effect of k_0a_o on Bandwidth Performance of TE_{11} to HE_{11} Mode Converters using Five Ring-Loaded Slots

(1) Maximum frequency determined by the TE_{11} mode in the output waveguide.
(2) Maximum frequency determined by EH_{12} mode excitation.

Value of k_0a_o	Return loss level >30 dB	Excitation of EH_{12} mode	TE_{11} mode in the corrugated output-guide	Usable bandwidth ratio (1)	(2)
2.4	$ka_o > 2.6$	$ka_o > 3.8$	$ka_o = 4.1$	1.6	1.5
2.9	$ka_o > 2.8$	$ka_o > 4.2$	$ka_o = 5.1$	1.8	1.5
3.4	$ka_o > 3.0$	$ka_o > 4.5$	$ka_o = 6.1$	2.0	1.5

approximately twice that of the slots in the output waveguide. The dashed curve XYZ in Fig. 3 is the contour of k_z/k for the fundamental mode when the slot depth is $\lambda/2$ at $k_ia_i=3.48$ (point Y), a_i being the input waveguide radius. (These parameter values correspond to the first slot used in the converter considered in detail in [1] and used for comparison with the performance of the ring-loaded converter in Section IV.) As the frequency and hence ka_i is increased beyond Y, the contour soon passes into the slow-wave region at Z. It has been found experimentally that the mismatch increases rapidly just prior to this condition. The other dashed curve VW is the contour of k_z/k for the corresponding higher order EH_{12} mode. Consider now the effect of this mode as it propagates through a converter with the inside radius a_i constant and equal to that of the output-waveguide radius a_o, with $k_0a_o=2.9$, as above. Propagation of this EH_{12} mode will not take place in the output waveguide until a value of ka_o corresponding to point D is reached. Hence, the dotted line WD repre-

sents the passage of this mode through the converter. For a ka_o value between V and D, the energy will be reflected from that section of the converter where cutoff for this mode occurs.

For converters having $k_i a_i$ considerably smaller than the example given in Fig. 3, the point Z will occur at a lower ka_i value than that at V. The upper frequency limit is then set by the deterioration in mismatch due to the onset of the EH_{11} slow wave.

The ring-loaded converter has a different characteristic from the conventional converter discussed above. It will be shown in the next section that the optimum performance of the ring-loaded converter occurs when the overall depth of the slots is constant and made equal to those in the corrugated output waveguide. The smaller slot depth (compared to that of the conventional converter) ensures a reduced frequency sensitivity. In addition, the first ring-loaded slot, which has a very narrow opening ($\sim 0.1 p_o$), represents a very low value of (capacitive) reactance over an extremely wide band compared to the conventional $\lambda/2$ slot (see Appendix and Fig. 6). Consequently, the contour of the fundamental mode in a waveguide using this type of slot lies just below that of the TE_{11} mode ($X_z = 0$), i.e., the mode is quasi-TE_{11}. The slow wave cannot be excited although there is the possibility of the EH_{12} (quasi-TM_{11}) mode being excited near $ka = 3.8$. However, the excitation of this mode at the first ring-loaded slot is likely to be negligible because of the very low impedance presented by this slot.

IV. Theoretical Performance of Ring-Loaded Slot Converters

In order to optimize the TE_{11} to HE_{11} mode match, and to obtain minimal excitation of EH_{1n} modes in the ring-loaded slot waveguide converter section (Fig. 2(a)), it is necessary to consider the effect and relative importance of several parameters. These include the number of slots L, the slot depths h_l and d_l, slot widths b_l and w_l, and pitch p_l ($= b_l + t_l$). The corrugated output-waveguide parameters are a_o, d_o, t_o, w_o, and p_o ($= t_o + w_o$). The slot depth d_o depends on a_o and the frequency f_0 where the HE_{11} mode is balanced. To a good approximation $d_o \approx (\lambda_0/4)\exp[1/(2.5k_0a_o)]$.[2] Three waveguide sizes were chosen viz., $k_0 a_o = 2.9$ (for which detailed computations were made), 2.4, and 3.4. The waveguide pitch p_o was set at $0.1\lambda_0$ and the slot width-to-pitch ratio δ was set at 0.75, both being values commonly used in corrugated waveguides. Note that although it is not a necessary limitation of our analysis, the output waveguide radius a_o and the input waveguide radius a_i were made equal in each case.

[2]This approximate expression for d_o has been deduced from the requirement that for the slots to present an infinite reactance to the HE_{11} mode, we must satisfy the equation [1]

$$J_1'[k_0 a_o] Y_1[k_0(a_o + d_o)] = Y_1'(k_0 a_o) J_1[k_0(a_o + d_o)]$$

An extensive theoretical parametric study was undertaken to consider all of the above factors in the design of ring-loaded slot mode converters. The main results of the investigation can be enumerated as follows.

1) The slot depths h_l and d_l: The slot depths should be maintained constant throughout with $d_l = d_o$ and $h_l \approx 2/3 d_l$. (These values are in substantial agreement with those used in the mode converter presented in [2].) Any variations from these values usually gave poorer results in all respects.

2) The number of slots L: At least five ring-loaded slots were necessary for satisfactory mode conversion. Increasing the number of slots gave some additional improvement in return loss performance at low frequencies ($f < f_0$). At those high frequencies where the EH_{12} mode can be excited, five ring-loaded slots produced a predicted power level of typically 1 percent or greater for this mode. By using 10 slots this power level was halved, but additional slots did not produce any further significant reduction in the level of the EH_{12} mode.

3) The pitch p_l: Since no advantage was found by altering the pitch p_l, it was fixed at the value p_o of the pitch in the corrugated output waveguide.

4) The slot widths b_l and w_l: Optimum mode conversion was achieved with w_l held constant and with b_l increasing linearly along the converter. The performance of the converter was insensitive to small changes in w_l, and hence it was made equal to w_o. To achieve maximum return loss performance, the width b_1 of the first slot should be less than $0.15 p_o$ (a value of $0.1 p_o$ has been used in this paper). Furthermore, at the last slot of the converter, where $w_L \to b_L$, it was necessary to retain the step in the slot, even if $w_L - b_L$ was as low as $0.015\lambda_0$, in order to maximize the return loss.

The optimized ring-loaded slot mode converter has, then, constant values for the pitch, the slot depths, and the width of the ring-loaded section of the slot. For a given number of slots L (where the use of five slots gives satisfactory mode conversion but up to 10 slots are required to minimize the level of the unwanted EH_{12} mode) the only variation in the converter is in the slot width b_l. Table II gives a summary of the parameters of the mode converter expressed in terms of the corrugated output waveguide used.

While the values of p_o and δ were fixed at $0.1\lambda_0$ and 0.75 for most of the analysis, small variations in p_o and δ were tried around these values and found not to significantly affect the mode conversion achieved. In addition, when the symmetrical slots shown in Fig. 2(a) were replaced by asymmetrical slots as in Fig. 1(a) (with, of course, the same values for h_l, d_l, w_l, and b_l) the results were essentially unchanged. The choice therefore between symmetrical and asymmetrical slots lies in their relative ease of manufacture.

Fig. 4 shows the predicted TE_{11} mode return loss for ring-loaded slot mode converters having 5, 10, and 20 slots

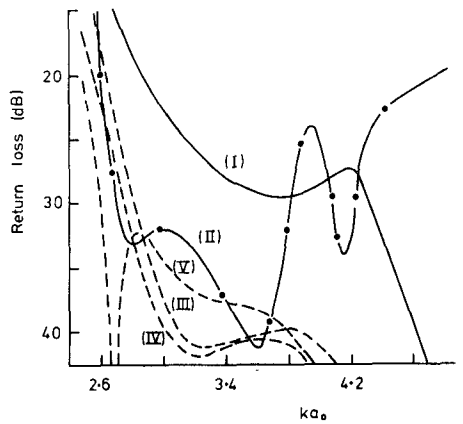

Fig. 4. Theoretical return loss of a number of corrugated converter sections placed between a smooth-walled cylindrical waveguide and a corrugated cylindrical waveguide of pitch $=0.1\ \lambda_0$, $\delta=0.75$, and $k_0a_o=2.9$. (I) Return loss without the converter section. (II) Optimized five-slot converter with constant width slots of varying depth as described in [1]. (III) $L=5$, (IV) $L=10$, (V) $L=20$: converter with L ring-loaded slots having constant depth.

TABLE II
OPTIMIZED PARAMETERS FOR A TE_{11} TO HE_{11} MODE CONVERTER
Parameters are expressed in terms of the corrugated output-waveguide parameters a_o, p_o, d_o, w_o, k_0 $(=2\pi/\lambda_0)$, where f_0 is the frequency at which the HE_{11} mode is in the balanced condition. L is the total number of ring-loaded slots.)

Parameter	Value
d_ℓ	$d_o\ \{\approx\frac{\lambda_0}{4}\ \exp\ [1/(2.5\ k_0a_o)]\}$
h_ℓ	$\frac{2}{3}\ d_o$
b_ℓ	$[0.1 + (\ell-1)\ (\delta-0.1)/L]\ p_o$
$p_\ell\ (=b_\ell+t_\ell)$	p_o
w_ℓ	w_o

(curves (III–V)) in which $k_0a_i=k_0a_o=2.9$. Also shown is the result when the converter is absent (curve (I)), and the return loss achieved by the mode converter described in [1] using five conventional slots of varying depth (curve (II)).[3] It is seen from the figure that the low-frequency performance of this converter can be equaled by a ring-loaded slot converter provided at least 10 slots are used. Increasing the number of ring-loaded slots gives further improvement in the low-frequency performance. The high-frequency match of the ring-loaded slot converters is seen to be clearly superior to that of the converter using varying depth slots. For this latter case, the return loss deteriorates seriously when $ka_o>3.8$, presumably owing to the excitation of the EH_{12} mode in the converter itself. The match deteriorates further near $ka_o=4.2$ owing to the onset of the EH_{11} slow-wave mode (see Fig. 3). Thus for return loss exceeding 30 dB, the bandwidth ratio is limited to 1.4 for this converter.

[3]Another possible means of mode conversion using conventional slots of fixed depth and variable width [2], [3] was shown in [1] to be ineffective.

The bandwidth performance of the ring-loaded slot converter with $k_0a_o=2.9$, and also for waveguide sizes either side of this value, is given in Table I. If the high-frequency performance is considered to be limited by EH_{12} mode propagation in the output waveguide then the overall bandwidth ratio performance achieved in all cases is 1.5 compared to 1.4 for the varying slot-depth converter. However, if the presence of the EH_{12} mode can be tolerated, the ring-loaded slot converter is seen to operate to considerably higher frequencies compared to the converter having varying depth slots. It is interesting to note that in order to optimize the low-frequency performance and hence the overall bandwidth it is found necessary to set the frequency at which the HE_{11} mode is balanced in the output waveguide close to the lower band edge (see Fig. 3). Consequently, for frequencies near and above the EH_{12} mode cutoff frequency, the HE_{11} mode will no longer be close to balance. The importance of this will depend on the particular application of the converter.

V. EXPERIMENTAL RESULTS

As a check on the validity of the theoretical analysis, a number of experiments to measure return loss were performed. An effective method of measuring directly the return loss of a converter terminated in a cylindrical corrugated waveguide has yet to be developed. The problem is to find a satisfactory arrangement for absorbing the energy in the corrugated waveguide without the excitation of spurious modes. Consequently, an indirect method as adopted in [1] has been used. This is to construct two identical mode-converter sections (the second one reversed) and connect them by a short length of corrugated waveguide. These three sections are then placed between two smooth-walled waveguides with the output guide terminated

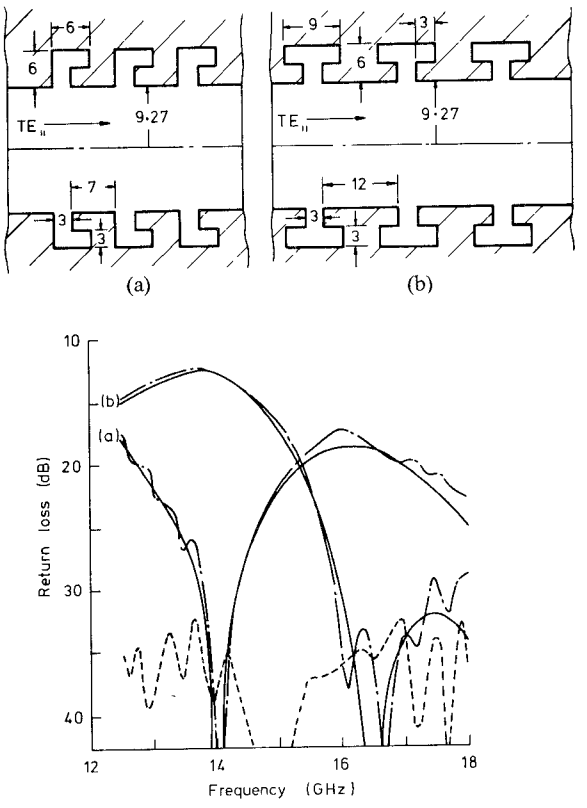

Fig. 5. Cross section of cylindrical waveguide with three ring-loaded slots which are: (a) asymmetrical; (b) symmetrical (all dimensions in millimeters); (c) return loss of (a) and (b) with the smooth output-waveguide terminated in a matched load. —— Theoretical; -·- measured; ---- measured inherent return loss in the experimental setup.

in a well-matched load. The mode converter, consisting of five ring-loaded slots, for which the theoretical performance is given by curve III in Fig. 4, was measured in this way using 11 slots in the uniform corrugated waveguide section. For values of ka_o up to 3, the theoretical and measured values of return loss were in good agreement, but at higher frequencies where the predicted return loss was well in excess of 30 dB, the measured result was masked by the inherent return loss of the measurement system.

As an alternative approach to validate the theoretical predictions, we measured the return loss of a circular waveguide system consisting of three identical ring-loaded slots placed between two smooth-walled waveguides with the output guide terminated in a well-matched load. Measured and theoretical results are shown in Fig. 5 for both asymmetrical and symmetrical slots. It is seen that agreement between experiment and theory (taking eight modes in the input waveguide) is generally very good.

VI. Conclusions

A detailed parametric study of a TE_{11} to HE_{11} mode converter consisting of a number of ring-loaded slots in a cylindrical waveguide has been investigated theoretically. It is shown that a minimum of five ring-loaded slots is required for acceptable mode conversion. With the aid of a mode chart, the conditions for propagation of the higher order EH_{12} mode in converters using ring-loaded or varying-depth slots are discussed. If excitation of the EH_{12} mode is to be avoided at higher frequencies, the converter bandwidth ratio for which the return loss exceeds 30 dB is restricted with ring-loaded slots to 1.5 and with varying depth slots to 1.4. However, the usable bandwidth of the converter with ring-loaded slots is considerably greater than this in applications where the low-level excitation of the unwanted EH_{12} mode is tolerable; furthermore, the upper-frequency limit increases as the waveguide radius increases and the low-frequency limit of operation is improved slightly by using more than five ring-loaded slots in the converter.

Appendix
Large Waveguide Diameter Approximation for Ring-Loaded Slot Behavior

When the waveguide diameter ka becomes large, the longitudinal surface reactance X_z of a corrugated waveguide can be determined approximately by considering each slot as a section of a short-circuited transmission line. The effect of slot parameters and frequency on X_z can then be easily determined. These calculations also illustrate the trend of behavior when the waveguide is small.

Consider the input ring-loaded slot in Fig. 2(a). The wide section of the slot has radial depth h_1 and impedance Z_1 proportional to w_1, whereas the narrow section has depth $h' = d_1 - h_1$ and impedance Z' proportional to b_1. Using the transmission line approximation, the normalized surface reactance X_z is given by

$$X_z = \delta \frac{\tan\beta_1 + \dfrac{b_1}{w_1}\tan\beta'}{1 - \dfrac{w_1}{b_1}\tan\beta_1 \tan\beta'} \tag{13}$$

where

$$\begin{aligned} \delta &= b_1/p_o \\ \beta_1 &= kh_1 \\ \beta' &= kh' = k(d_1 - h_1) \\ k &= 2\pi/\lambda. \end{aligned}$$

When ka is large, the general equation for the reactance of a ring-loaded slot given by (8) of [3] reduces to (13) above if the shunt reactance resulting from the discontinuity in slot widths is ignored. In addition, for a constant-width slot where $\beta' = 0$, (13) reduces to the standard approximation $X_z = \delta \tan\beta_1$ for ka large.

Fig. 6 shows the solution of (13) for both conventional constant-width slots, and ring-loaded slots. For a converter using a conventional one-half-wavelength input slot, the reactance is seen to vary rapidly with frequency and to remain small only over a very narrow band. On the other hand, the ring-loaded input slot presents a very low reactance over a very wide band. Compared to a conventional slot having the same depth, the frequency at which $X_z \to \infty$ is considerably lower for the ring-loaded slot. The frequency at which $X_z = 0$ for the ring-loaded slot is a function of the

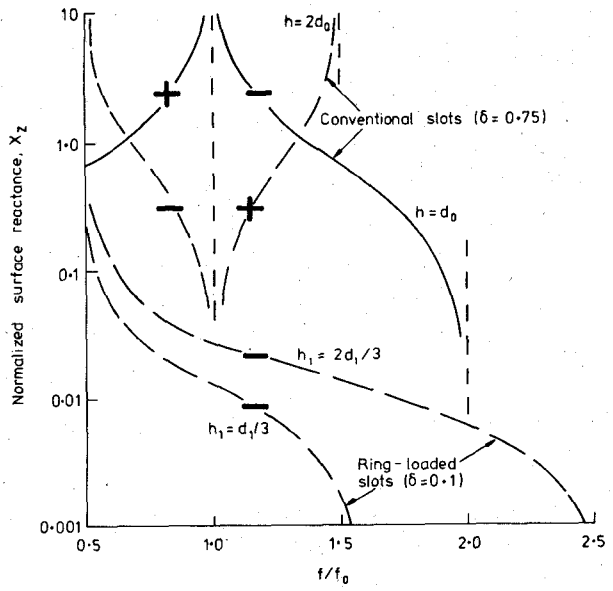

Fig. 6. Large waveguide diameter approximation for normalized surface reactance of a corrugated waveguide having conventional and ring-loaded slots plotted as a function of frequency. f_0 is the resonant frequency of the quarter-wave slots (depth d_o) in the output waveguide. —— Output corrugated waveguide ($h = d_o$, $\delta = 0.75$); ---- input half-wavelength slot of conventional converter ($h = 2d_o$, $\delta = 0.75$); –– input slot of ring-loaded converter ($d_1 = d_o$, $\delta = 0.1$) for two cases: $h_1 = 2d_1/3$ and $d_1/3$ (see Fig. 2).

depth ratio h_1/d_1 of the slot. Using $h_1 \approx 2d_1/3$ gives close to maximum bandwidth for the ring-loaded slot, whereas minimum bandwidth results if $h_1 \approx d_1/3$. This trend is in close agreement with that predicted in references [2] and [3] for small waveguide diameters using a more exact analysis.

Acknowledgment

The authors are indebted to K. J. Greene, who carried out the measurements, and to the craftsmen in the CSIRO Division of Radiophysics machine shop, particularly K. J. Hodgson, for machining the corrugated waveguide sections.

References

[1] G. L. James, "Analysis and design of TE_{11} to HE_{11} corrugated cylindrical waveguide mode converters," *IEEE Trans. Microwave Theory Tech.* vol. MTT-29, pp. 1059–1066, Oct. 1981.

[2] Y. Takeichi, T. Hashimoto, and F. Takeda, "The ring-loaded corrugated waveguide," *IEEE Trans. Microwave Theory Tech.*, vol. MTT-19, pp. 947–950, Dec. 1971.

[3] F. Takeda and T. Hashimoto, "Broadbanding of corrugated conical horns by means of the ring-loaded corrugated waveguide structure," *IEEE Trans. Antennas Propagat.* vol. AP-24, pp. 786–792, Nov. 1976.

[4] B. MacA. Thomas and H. C. Minnett, "Modes of propagation in cylindrical waveguides with anisotropic walls," *Proc. IEE*, vol. 125, pp. 929–932, Oct. 1978.

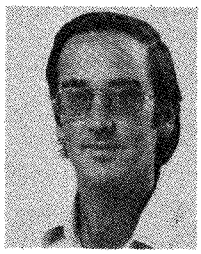

Graeme L. James was born in Dunedin, New Zealand, on September 11, 1945. He received the B.E. and Ph.D. degrees in electrical engineering from the University of Canterbury, Christchurch, New Zealand, in 1970 and 1973, respectively.

Between 1973 and 1976 he was a post-doctoral Fellow with the Department of Electrical and Electronic Engineering, Queen Mary College, London, England, where he was involved in a number of projects concerned with electromagnetic scattering and diffraction and wrote his book *Geometrical Theory of Diffraction for Electromagnetic Waves*. Since June 1976 he has been with the Division of Radiophysics, Commonwealth Scientific and Industrial Research Organization, Sydney, Australia where he has been mainly concerned with research into high performance microwave antennas.

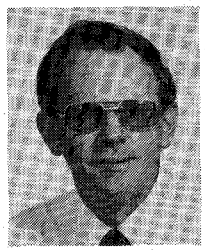

Bruce M. Thomas (M'68–SM'73) was born in Melbourne, Australia in 1937. He received the B.E. and Ph.D. degrees in electrical engineering from the University of Melbourne in 1959 and 1964, respectively.

In 1964 he joined the Division of Radiophysics, Commonwealth Scientific and Industrial Research Organization in Sydney. His main interest has been the research and development of high-efficiency, low cross-polarization horns for radio astronomy and satellite communications. He is the author of some 30 papers in this field. For the last few years he has been involved in the upgrading of several Earth Station antennas for the Overseas Telecommunications Commission, Australia.

Dr. Thomas is a Member of the Institution of Electrical Engineers, London, a Fellow of the Institution of Radio and Electronics Engineers, Australia and a member of the Antennas and Propagation Society of the IEEE.